Space Weather of the Heliosphere: Processes and Forecasts
Proceedings IAU Symposium No. 335, 2017
C. Foullon & O.E. Malandraki, eds.

doi:10.1017/S1743921318000443

Acceleration of Solar Wind Particles Passing through the 3D Heliospheric Current Sheet

Valentina V. Zharkova

Department of Mathematics, Physics and Electrical Engineering, University of Northumbria, Newcastle upon Tyne, NE1 8ST, UK
email: valentina.zharkova@northumbria.ac.uk

Abstract. Additional acceleration of protons and electrons passing through a 3D reconnecting current sheet (RCS) of the solar corona and heliosphere is investigated with PIC approach. The simulation confirms spatial separation of electrons and protons and generation of a polarisation electric field induced by separated particles. In the heliospheric current sheet with a weak magnetic field there are two populations of particles: transit and bounced. The transit particles (both protons and electrons) are accelerated to high energies while the bounced electrons fail to reach the midplane. Instead they form an electron cloud of horseshoe or medallion types at some distance D from its midplane, which is larger for bigger guiding field magnitudes. These energetic electrons and protons appearing near the HCS boundaries can be a great danger for the satellites crossing the sector boundaries.

Keywords. Sun: flares, plasmas, acceleration of particles, magnetic field

1. Introduction

The interplanetary magnetic field (IMF) in the heliosphere is divided into two sectors of the open magnetic field lines with the opposite magnetic field polarities separated by the equatorial plane providing a magnetic field reversal known as the sector boundary (SB). The latter is considered to be the heliospheric current sheet (HCS), which governs the magnetic field reversals from and toward the Sun along Parker′s spiral (see http://wso.stanford.edu/gifs/HCS.html).

Simulations of particle trajectories were carried out by using a test particle approach in a 3D magnetic configuration with the guiding field emulating a simple case of magnetic reconnection for a constant reconnection electric field (Zharkova and Gordovskyy 2004) or for those enhanced near the magnetic X-nullpoint due to anomalous resistivity (Wood and Neukirch 2005). Zharkova and Gordovskyy (2004) and Zharkova and Agapitov (2009) showed that the trajectories of particles with the opposite charges (electrons or protons) can be either fully symmetric or strongly asymmetric towards the midplane of the RCS depending on the ratio between the magnetic field components.

As a result, some fraction of the released magnetic energy is transformed into kinetic energy of accelerated particles. The energy spectra of these particles also depend on a magnetic field topology, electric field strength and the magnitude of a transverse magnetic field. Accelerated particles gain energies up to 100 keV for the electrons and up to a few tens MeV for the protons (Zharkova and Gordovskyy 2005; Wood and Neukirch 2005; Zharkova and Agapitov 2009).

Recent study with particle-in-cell (PIC) of particle acceleration in the 3D heliospheric current sheet with low magnitudes of magnetic field relevant to the interplanetary magnetic field at the Earth orbit (Zharkova and Khabarova 2012) allowed to provide the plausable interpretation of the energies and pitch angle distributions of electrons and protons after their passage through the HCS.

2. Description of the model

A PIC approach was used for the simulation of particle acceleration in a 3D reconnecting current sheet with simple magnetic field topology and ambient particle densities relevant to the HCS.

The simulation domain is a small part of the RCS (see model in Siversky and Zharkova (2009) where periodic boundary conditions are used to contain the full trajectories of accelerated particles. The main component B_z depends on x as follows: $B_z(x) = -B_{z0}\tanh\left(\frac{x}{L_x}\right)$. Similar to Zharkova and Gordovskyy (2004), the B_x component is assumed to be constant inside the simulation domain, i.e. $B_x = -B_{x0}$. The guiding (out-of-plane) magnetic field B_y is maximal in the midplane and vanishes outside the RCS: $B_y(x) = B_{y0}\mathrm{sech}\left(\frac{x}{L_x}\right)$. Particles are considered accelerated by the reconnection electric field E and to generate their own electric and magnetic fields as described by Siversky and Zharkova (2009).

Simulations are carried out for the following current sheet parameters: the main component of the magnetic field $B_{z0} = 10^{-3}$ T, the current sheet half-thickness $L_x = 1$ m, the drifted electric field $E_{y0} = 250$ V/m and the guiding, B_{y0}, and transverse, B_{x0}, components of the magnetic field are selected to range from $(0.1 - 10) \times 10^{-4}$ T to cover acceleration at the various parts of the RCS.

3. Results

The PIC simulations have shown that the induced magnetic field $\tilde{\mathbf{B}}$ is much smaller than the background $\mathbf{B_z}$. On the other hand, the electric field $\tilde{\mathbf{E}}_\mathbf{x}$, called a polarization field, induced by the separation of electrons from protons is much larger than the reconnection (drifted) field E_y as pointed out by Zharkova and Agapitov (2009) and Siversky and Zharkova (2009). The polarization electric field $\tilde{E}_x$, which is perpendicular to the current sheet, leads to a local non-neutrality of the plasma, which becomes stronger if B_{x0} decreases, or B_{y0} increases.

Electrons entering from the $x < 0$ semi-space reveal the dynamics similar to those of the 'transit' protons, e.g. drifting towards the midplane, becoming accelerated and ejected to the $x > 0$ semi-space. However, the polarization field $\tilde{E}_x(x)$, which extends beyond the current sheet and has a component parallel to the magnetic field B_z decelerates the ejected electrons and returns them back to the point where they entered the acceleration region (see Figure 1a). While transit electrons are accelerated at the midplane, ejected from it into the interplanetary space without return because of a weak magnetic field.

The observations of solar wind energetic electrons with energies above 2 keV often reveal that the locations of their motion reversals do not always coincide with the locations (and times) of the magnetic field reversals in the HCS, or sector boundary crossings (SBC) (Kahler and Lin 1994, 1995). According to Crooker *et al.* (2004a,b), the mismatch between the SBC allegedly indicated by a change of electrons pitch angles occuring in one location (see Figure 1b) and the change of a sign and magnitude of the IMF occurring in another location is caused by entangling of the large-scale magnetic field.

However, these discrepancies in spatial observations of the electrons in a vicinity of the HCS can be explained in much more simple and logical manner by rather dynamic

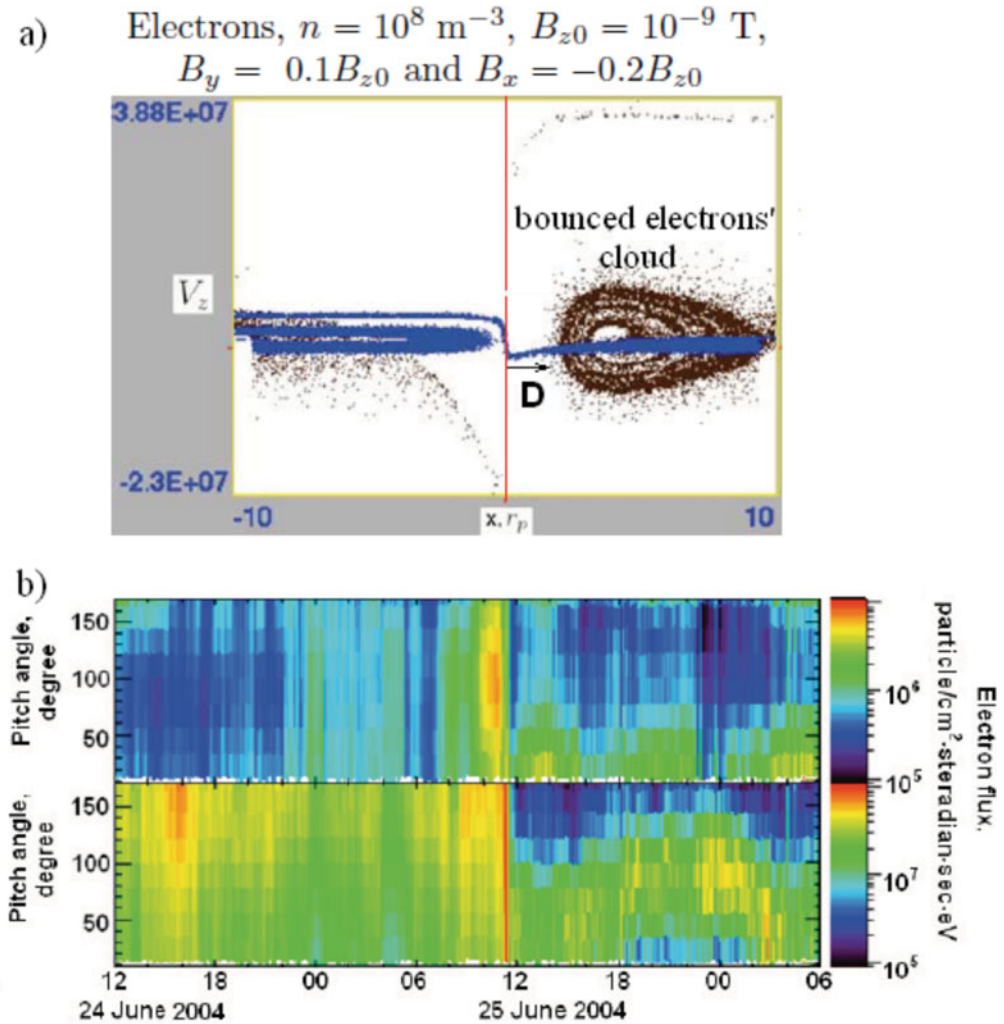

Figure 1. Comparison of a) accelerated electron (black dots) and proton (blue dots) distributions simulated for strong guiding field with PIC with respect to the current sheet midplane (X=0) and b) observed energy and pitch angle distributions of electrons passed through the HCS. Note that simulated distributions of the bounced electrons (for X> 0) do not reach the midplane but turned back at some distance D from it. This causes the pitch angle distributions shown in b) with the variations of a pitch angle from 0 to 180° similar to the simulated variation in a).

physical conditions in the HCS caused by the ongoing magnetic reconnection and correspondence of SBC to the HCS midplane. In this case electrons become accelerated as shown in Figure 1a to form the transit electrons leaving the current sheet with energies of a few hundreds of eV as measured, and the bounced electrons with energies of a few tens of eVs, which are turning by 180 degrees from their initial motion (towards the SB, or midplane of the HCS) from the HCS at some distance D from its midplane (SB for HCS).

Remarkably, the population of bounced electrons forms either the horseshoe or medallion shapes for weaker IMF magnitudes of 10^{-9} nT (see Figure 1a). This resembles the pitch angle distributions often observed in the interplanetary space (Figure 1b). The

https://doi.org/10.1017/S1743921318000443 Published online by Cambridge University Press

distance D, at which the electrons change their pitch angles is larger for a bigger guiding field magnitude that fits rather well the observations (see Table 1 in Zharkova and Khabarova 2012).

The analysis of the measurements near the SBC from the Interball-1 spacecraft and Wind SWE data (1995−2005) revealed rather peculiar profiles of the solar wind velocities V across the HCS (see Figure 5 in Zharkova and Khabarova 2012). The unexplained decrease of the solar wind velocity observed 1-3 days before the SBC and a sharp increase of this velocity 1-3 days after the SBC is defined by the polarisation electric field. Only in about 50% of cases the ion velocity dostributions can be assigned to a presence of the co-rotating interaction region (CIR) approaching the HCS, observed though after the SBC. Hence, the other 50% cases are to be associated with the particles accelerated during their sector boundary crossing. The observed asymmetric velocity profiles of the solar wind ions during their crossing of the SB are likely to be caused by the effect of an asymmetric polarisation electric field induced by the separation of accelerated electrons and protons with respect to the current sheet midplane, or SB (Zharkova and Khabarova 2012).

4. Conclusions

The PIC simulation has shown that accelerated particles produce a strong polarisation field, $\tilde{E}_x$, caused by the separation of accelerated particles across the current sheet. This process results in formation of peculiar velocity profiles of ions following the polarisation electric field and of electron clouds in the form of a 'horse shoe' or 'medallion' well before the electrons can reach the current sheets. The clouds disappear only when protons gain sufficient energy to leave the model RCS while dragging electrons with them.

References

Crooker, N. U., Forsyth, R., Rees, A., Gosling, J. T. & Kahler, S. W. 2004a, *Journal of Geophysical Research (Space Physics)*, 109, A06110

Crooker, N. U., Huang, C.-L., Lamassa, S. M., *et al.* 2004b, *Journal of Geophysical Research (Space Physics)*, 109, A03107

Gosling, J. T., Eriksson, S. & Schwenn, R. 2006a, *Journal of Geophysical Research (Space Physics)*, 111, A10102

Gosling, J. T., McComas, D. J., Skoug, R. M. & Smith, C. W. 2006b, *Geophysics Research Letters*, 33, L17102

Kahler, S. & Lin, R. P. 1994, *Geophysics Research Letters*, 21, 1575

Kahler, S. W. & Lin, R. P. 1995, *Solar Physics*, 161, 183

Lin, R. P., Ko, Y. K., Sui, L., *et al.* 2005, *Astrophysical Journal*, 622, 1251

Priest, E. & Forbes, T. 2000, *Magnetic Reconnection* (Magnetic Reconnection, by Eric Priest and Terry Forbes, pp. 612. ISBN 0521481791. Cambridge, UK: Cambridge University Press, June 2000.)

Siversky, T. V. & Zharkova, V. V. 2009, *Journal of Plasma Physics*, 75, 619

Verboncoeur, J. P. Langdon, A. B. & Gladd, N. T. 1995, *Comp. Phys. Comm.*, 87, 199

Wood, P. & Neukirch, T. 2005, *Solar Physics*, 226, 73

Zharkova, V. V. & Gordovskyy, M. 2004, *Astrophysical Journal*, 604, 884

Zharkova, V. V. & Gordovskyy, M. 2005, *Monthly Notices of the Royal Astronomical Society* **356**, 1107–1116.

Zharkova, V. V. & Agapitov, O. V. 2009, *Journal of Plasma Physics*, 75, 159

Zharkova, V. V. & Khabarova, O. V. 2012, *Astrophysical Journal*, Vol. 752, 35

Zharkova, V. V. & Khabarova, O. V. 2015, *Annales Geophys.*, 33, 457